Journal of Nuclear Materials 393 (2009) 134–140

Contents lists available at ScienceDirect

Journal of Nuclear Materials

journal homepage: www.elsevier.com/locate/jnucmat

Self-radiation damage in plutonium and uranium mixed dioxide

Masato Kato [a,*], Akira Komeno [a], Hiroki Uno [b], Hiromasa Sugata [b], Nobuo Nakae [a,c], Kenji Konashi [d], Motoaki Kashimura [a]

[a] Japan Atomic Energy Agency, 4-33 Muramatu, Tokai-Mura, Naka-gun, Ibaraki 319-1194, Japan
[b] Inspection Development Company, 4-33 Muramatu, Tokai-Mura, Naka-gun, Ibaraki 319-1194, Japan
[c] Japan Nuclear Energy Safety Organization, TOKYU REIT Toranomon Bldg, 3-17-1, Toranomon, Minato-ku, Tokyo 105-0001, Japan
[d] Tohoku University, 2145-2, Narita, Oarai-machi, Ibaraki 311-1313, Japan

ARTICLE INFO

Article history:
Received 24 April 2008
Accepted 27 May 2009

PACS:
61.72.Cc
61.82.−d

ABSTRACT

In plutonium compounds, the lattice parameter increases due to self-radiation damage by α-decay of plutonium isotopes. The lattice parameter change and its thermal recovery in plutonium and uranium mixed dioxide (MOX) were studied. The lattice parameter for samples of MOX powders and pellets that had been left in the air for up to 32 years was measured. The lattice parameter increased and was saturated at about 0.29%. The change in lattice parameter was formulated as a function of self-radiation dose. Three stages in the thermal recovery of the damage were observed in temperature ranges of below 673 K, 673–1073 K and above 1073 K. The activation energies in each recovery stage were estimated to be 0.12, 0.73 and 1.2 eV, respectively, and the corresponding mechanism for each stage was considered to be the recovery of the anion Frenkel defect, the cation Frenkel defect and a defect connected with helium, respectively.

© 2009 Elsevier B.V. All rights reserved.

1. Introduction

Nuclear fuels are left under non-operating conditions during periodic inspections or when there is trouble in the plant. In some cases fresh fuels are also kept for several years until loaded into the core. In the case of plutonium and uranium mixed oxide (MOX) fuels used as fast reactor fuels, radiation damages accumulate in the fuel pellets during the storage time due to α-particles produced from spontaneous decay of actinide elements at low temperature. In several studies [1–4], the radiation damages were found to affect physical properties of the pellets, i.e., lattice parameter, electrical resistivity and thermal conductivity. Such variations of physical properties might affect irradiation behavior when the reactor is restarted.

Studies of radiation damage of PuO_2, AmO_2 and CmO_2 have been carried out [5–11]. The following relationship between lattice parameter and storage time was obtained for $^{238}PuO_2$, $^{239}PuO_2$, $^{240}PuO_2$, $^{241}AmO_2$, $^{244}CmO_2$:

$$\Delta a/a_0 = A_1 \times \exp\{1-(-B_1 \times \lambda \times t)\}, \tag{1}$$

where a_0 is the lattice parameter just after preparation, Δa is the increment of lattice parameter caused by self-radiation, A_1 and B_1 are constants, λ is the decay constant of actinide isotope and t is time for storage. However, it should be pointed out that Eq. (1) cannot be applied directly to plutonium and uranium mixed oxide (MOX) because plutonium includes several isotopes having different decay constants.

Weber [12–14] examined thermal recovery of lattice defects in α-irradiated UO_2 and found three recovery stages from which it was concluded that the three stages corresponded to recoveries of the three different types of defects, i.e., anion Frenkel defects, cation Frenkel defects and defects composed of isolated helium trapped in a vacancy. There are no data on recovery for MOX. In this work, the rate of the lattice expansion and the thermal recovery due to the self-radiation damage for MOX were investigated.

2. Experimental

2.1. Sample preparation

The mixed oxides with various Pu contents were prepared by mechanical blending method [15]. The mixed oxide sample characteristics are summarized in Table 1. Samples A–D were prepared from the same material powders of UO_2 and MOX with plutonium content of 48.6 wt%, which was obtained by co-conversion of uranium plutonium mixed nitrate. Plutonium isotope ratios of the samples are shown in Table 2 together with half-life and decay constant of α-decay. The samples were sintered at 1973 K for 2 h

---

[*] Corresponding author. Tel.: +81 29 282 1111; fax: +81 29 282 9473.
E-mail address: kato.masato@jaea.go.jp (M. Kato).

0022-3115/$ - see front matter © 2009 Elsevier B.V. All rights reserved.
doi:10.1016/j.jnucmat.2009.05.020

Table 1
Samples.

Sample	Pu content (wt%)	Density (% TD)	O/M ratio		Storage time (days)	Sample form during storage
			After sintering	After storage		
Sample A	29.7	95.1	2.00	2.00	626	Powder
Sample B	39.9	94.8	2.00	2.00	626	Powder
Sample C	45.0	94.7	2.00	2.00	626	Powder
Sample D	48.6	94.9	2.00	2.00	626	Powder
Sample E	17.4	92.6	1.99	1.99	11 688	Pellet
Sample F	18.9	92.5*	1.99	1.99	5903	Pellet
Sample G	30.0	85.0*	1.97	2.01	8794	Pellet
Sample H	27.9	92.8*	1.97	1.97	5478	Pellet

* Samples were prepared by use of pore former Avicel.

Table 2
Isotope ratios of samples [Isotope/(Pu + Am)], half time and decay constant.

	Half-life (year)	Decay constant (S^{-1})	Isotope ratio (%)*				
			Samples A–D	Sample E	Sample F	Sample G	Sample H
Pu-238	87.74	2.505×10^{-10}	1.07	1.10	0.97	1.07	1.16
Pu-239	24 110	9.116×10^{-13}	60.42	65.65	65.59	65.00	65.15
Pu-240	6563	3.349×10^{-12}	25.34	22.83	22.78	23.05	23.12
Pu-241	3.2×10^{5}	6.869×10^{-14}	6.14	6.55	3.11	4.04	6.43
Pu-242	3.733×10^{5}	5.888×10^{-14}	4.31	3.87	3.87	4.13	4.14
Am-241	432.1	5.086×10^{-11}	2.73	2.91	3.67	2.70	3.49

* At the time of fabrication.

in flowing gas of Ar/5% H_2 and then annealed at 1123 K for 5 h under the condition that $\Delta\bar{G}_{O_2} \cong -400$ kJ/mol to adjust O/M to 2.00. Pellet samples were crushed and milled to powder and left in air for about 2 years before measuring the lattice parameter. It was confirmed that O/M ratio of the samples did not change and remained as 2.00 ± 0.005 for about 2 years. A portion of sample D was stored in air as pellets and was provided for helium analysis.

The pellets of samples E–H were fabricated in 1975, 1991, 1983 and 1992, respectively for irradiation tests and were stored in sample containers sealed in air. The O/M ratios and isotope ratios of the samples are shown in Tables 1 and 2. The O/M ratios were adjusted to hypo-stoichiometric composition (1.97–1.99). In the case of sample G, the O/M ratio changed from 1.97 to 2.01 after 15 years. No change of the O/M was observed for the other samples. The homogeneity of plutonium was confirmed by the α-autoradiography method and electron probe micro analyzer. There was no significant plutonium enriched zone in the samples.

2.2. Analysis of samples

Isothermal annealing was done to samples A–D having plutonium contents of 29.7, 39.9 and 48.6 wt% at 473–1473 K for 2 h. Sample D was annealed for 4 and 6 h at temperatures of 673, 873, 1073 and 1273 K. Number of annealing per sample was just one time. Oxygen partial pressure during annealing was controlled by flowing $Ar/H_2/H_2O$ gas in order to keep the O/M ratio constant. A thermal gravimeter was used to check the change of the O/M ratio during annealing.

The lattice parameter of samples, after storage, was measured by X-ray diffraction (Rigaku RINT-1100). Diffraction patterns were taken in 2θ range from 110° to 145° using the Cu–Kα ray. Lattice parameter was determined by Rietveld analysis, which allows automatic evaluation of the lattice parameter.

The helium analysis was done for sample D. Samples were heated at 973, 1073, 1173, 1273 and 1373 K for 0.5 h in vacuum. The gas released from the samples was analyzed by mass spectrometer (ULVAC Mass Mate 100).

3. Results

3.1. Lattice parameter change

Analyses of X-ray diffraction patterns show that all samples have the single fcc structure. Fig. 1 shows variation of $\Delta a/a_0$. Lattice parameters increase with time and seem to saturate for long-time storage. As seen in Fig. 1, the effect of the storage on lattice expansion is enhanced in the case of the sample with high plutonium content. This can be explained as production rate of lattice defects is related to plutonium content.

Lattice expansion of actinide oxides such as $^{238}PuO_2$, $^{239}PuO_2$, $^{241}AmO_2$ and $^{243}CmO_2$ has been studied by several groups

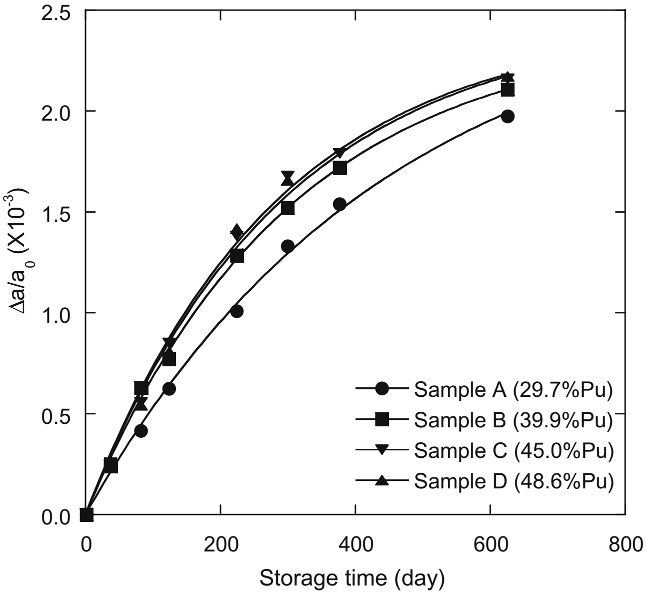

Fig. 1. The change ratio of lattice parameter as a function of storage time.

[1,3,4,8–11] and they reported that the fractional increase of lattice parameter was well represented by Eq. (1). Eq. (1) can be applied to oxides containing only one actinide isotope. However, MOX samples have multi-isotopes of plutonium with various isotopic compositions. The effective decay constant (λ' of the MOX fuel is considered in this work:

$$\lambda' = C_{\mathrm{Pu}} \sum \lambda_i C_i, \tag{2}$$

where C_{Pu} is plutonium content, λ_i is decay constant of plutonium isotope and C_i is plutonium isotopic composition. A total of four kinds of plutonium isotopes and one americium isotope are considered here: ^{238}Pu, ^{239}Pu, ^{240}Pu, ^{241}Pu and ^{241}Am. The decay of ^{241}Pu to ^{241}Am is not considered in estimating the effective decay constant in Eq. (2), since the influence on λ' is evaluated as about 1% during storage for 2 years.

The $\Delta a/a_0$ values plotted in Fig. 1 are re-plotted in Fig. 2(a) as a function of $\lambda' t$. The figure shows that the $\Delta a/a_0$ of samples with various Pu contents are reproduced with a single curve as a function of $\lambda' t$, which corresponds to self-radiation dose, in other words, α-particle dose. Fig. 2(b) shows the relative expansion of $\Delta a/a_0$ for samples E–H as a function of $\lambda' t$. Using λ' for λ in Eq. (1), a modified equation is derived as follows:

$$\Delta a/a_0 = A_2(1 - \exp(B_2 \lambda' t)), \tag{3}$$

where $A_2 = 2.9 \times 10^{-3}$ and $B_2 = -12\,000$.

The values of constants A_2 and B_2 are obtained by fitting Eq. (3) to the data. As shown in Fig. 2(b), Eq. (3) can reproduce experimental data very well. This fact validates the idea of the effective decay constant, in evaluating lattice expansion of MOX after storage. According to Eq. (3), the relative expansion $\Delta a/a_0$, reaches a saturation value after a sufficient storage time, and that value is expressed by the constant A_2. So, the lattice parameter of MOX is saturated after the increase of about 0.29%.

3.2. Thermal recovery

Fig. 3 shows the effect of isothermal annealing for 2 h on lattice parameter. All data were tested by use of fresh samples. The vertical axis of Fig. 3 is recovery fraction, which is expressed by the following relation:

$$F = (a_S - a_{HT})/(a_S - a_O) = (a_S - a_{HT})/\Delta a, \tag{4}$$

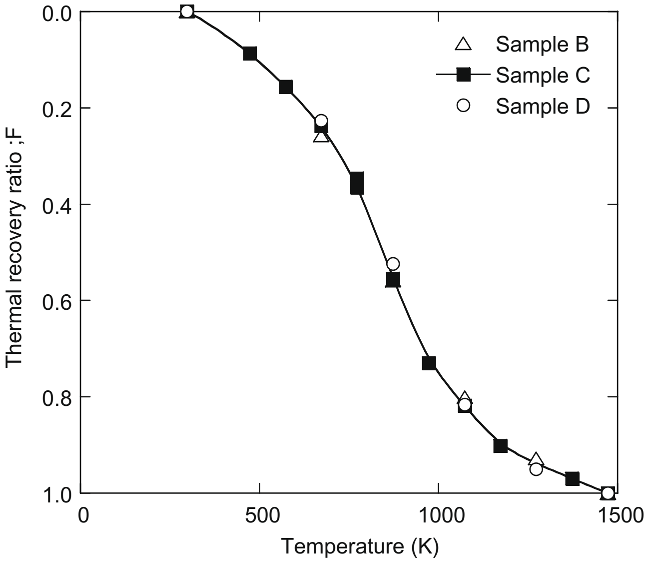

Fig. 3. Thermal recovery of MOX.

where a_S and a_{HT} are lattice parameters before and after annealing, respectively.

Thermal recovery behavior of MOX with different plutonium contents might be correlated to each other and the behavior can be expressed by a single curve as shown in Fig. 3. No plutonium content dependence on thermal recovery is observed. The lattice expansion due to self-radiation is completely recovered by annealing to 1473 K. The thermal recovery of MOX is also compared with recovery of the other actinide oxides in Fig. 4. The thermal recovery of UO_2, PuO_2 and $(U,Th)O_2$ might be occurring in three stages. Weber [13] reported that the recovery occurred in three stages in UO_2. However, the recovery stages in the thermal recovery of MOX were not clear.

Sample D was annealed for 2, 4 and 8 h, and its lattice parameters were measured after the annealing. As shown in Fig. 3, the thermal recovery of the sample annealed at 673 K for 2 h was estimated to be $F = 0.24$. In the Fig. 5, the thermal recovery at 673 K was not observed until 8 h. These observation results suggested

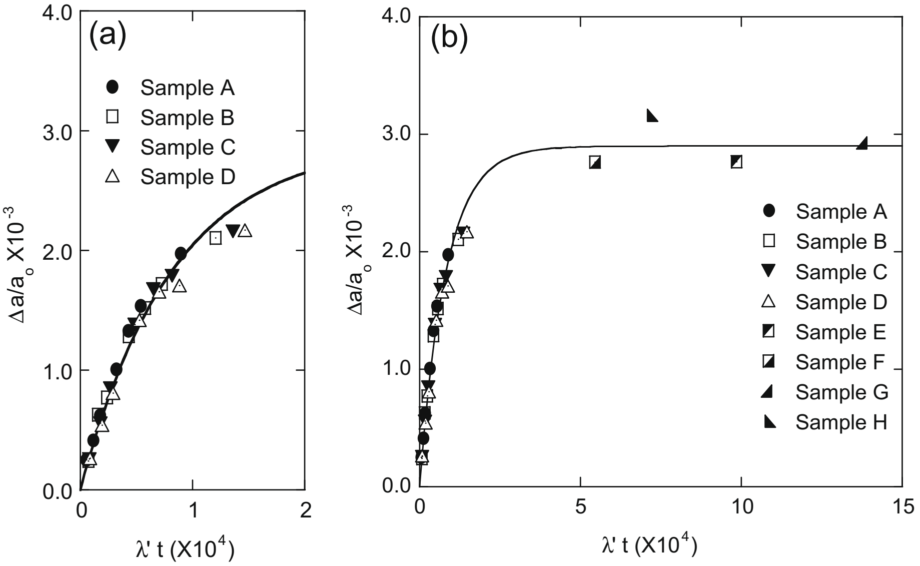

Fig. 2. Lattice expansion of MOX dependence on $\lambda' t$.

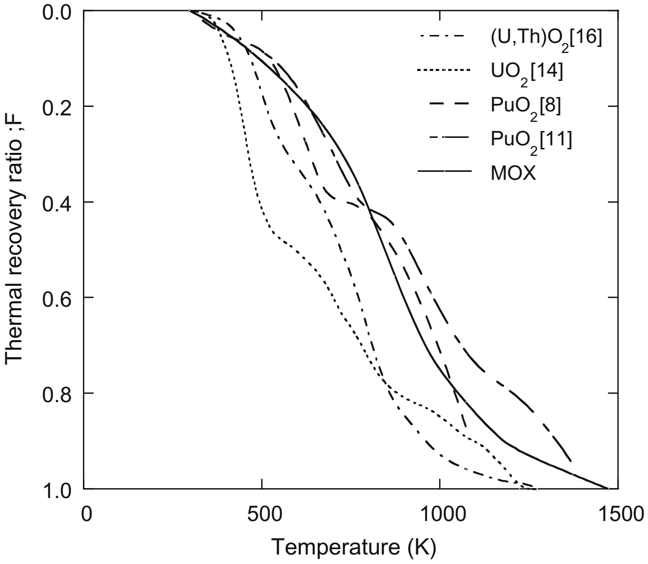

Fig. 4. Comparison of thermal recovery.

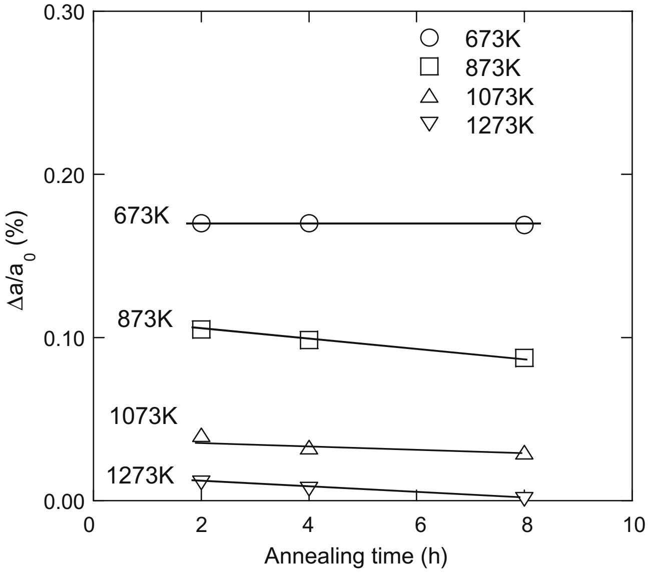

Fig. 5. Comparison of thermal recovery.

Table 3
Results of gas analysis in MOX kept for 2 years.

Annealing temperature (K)	Total amount of released gases (μl)	Detected gases
973	0.7	H, H_2, N, O, H_2O, N_2, CO, O_2, CO_2
1073	1.0	H, H_2, H_2O, CO
1173	1.5	H, H_2, H_2O, CO
1273	4.1	H, H_2, He, H_2O, CO
1373	6.5	H, H_2, H_2O, CO

that some recovery process existed in the temperature range of less than 673 K, and the recovery at 673 K occurred in a short time of less than 2 h.

If the recovery was caused by elementary process, the recovery rate increased with temperature. However, the recovery proceeded slowly at 873 K and its rate decreased again at 1073 K. As observed above, the thermal recovery rate did not increase with increasing temperature. These results suggested that thermal recovery in MOX occurred in at least three kinds of process which were occurred in the temperature ranges of less than 673 K, 673–1073 K and more than 1073 K. In previous works [8,11,14,16], it was reported that the thermal recovery of PuO_2, UO_2 and $(U,Th)O_2$ occurred in three stages, which were explained by the recoveries of three kinds of the lattice defects, anion Frenkel defects, cation Frenkel defects and defects composed of isolated helium trapped in a vacancy occurred. Their data were shown in Fig. 4. The temperature ranges in which three kinds of recovery occurred are almost same with those of the recoveries observed in MOX. Therefore, it is assumed that the thermal recovery in MOX proceeded by three kinds of process, and the three recovery processes are called "Stage I", "Stage II" and "Stage III".

Total amount of gases and the gases detected are shown in Table 3. The amount of gases released after heating increases at temperature over 1173 K and the main detected gases are H_2, H_2O, CO and CO_2. The release of helium gas is only detected at 1273 K, which occurs in the temperature region of Stage III. Therefore, it is considered that the recovery is caused by migration of helium.

4. Discussion

4.1. Lattice expansion and self-radiation damage

The dependence of self-radiation dose on fractional increase of lattice parameter of MOX is shown in Fig. 6 together with that of other actinide oxides [8,11,13,16]. The data for dose dependence

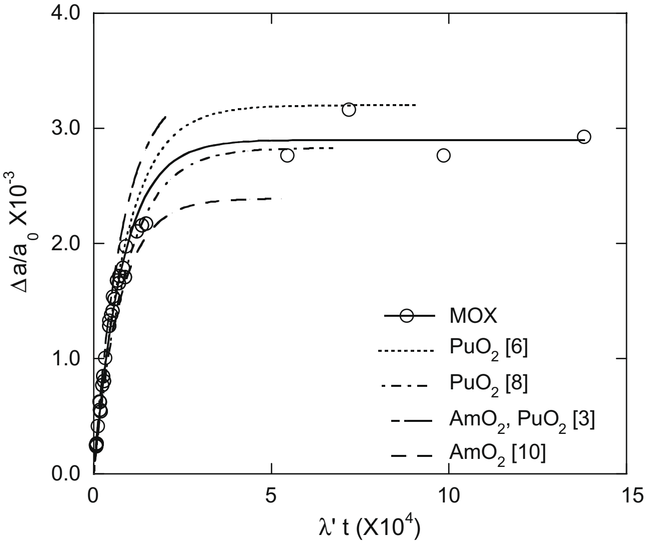

Fig. 6. Thermal recovery dependence on annealing time.

Table 4
Comparison of constants *A* and *B* in Eq. (1).

	A	*B*
MOX	2.90E−03	1.22E+04
$^{238}PuO_2$ [8]	2.83E−03	1.08E+04
$^{238}PuO_2$ [4]	3.20E−03	1.11E+04
$^{239}PuO_2$ [1]	3.90E−03	0.87E+04
$^{239}PuO_2$, $^{238}PuO_2$, $^{241}AmO_2$ [3]	3.38E−03	1.23E+04
$^{241}AmO_2$ [10]	2.39E−03	1.34E+04
$(U,Th)O_2$ [16]	8.4E−3	–
UO_2* [12]	4.5–7.9E−3	–

* Single crystal irradiated with α-particles.

Table 5
Comparison of activation energy in each thermal recovery.

	Stage I (eV)	Stage II (eV)	Stage III (eV)	References
MOX	0.12	0.73	1.2	This work
$^{238}PuO_2$	0.15 ± 0.05	–	–	[17]
PuO_2	0.20	–	–	[6]
PuO_2	0.23	–	–	[8]
UO_2	1.5	2.2		[12]

of lattice parameter are fitted by a modified Eq. (1) and the two constants A and B appearing in Eq. (1) can be obtained; those values are shown in Table 4. As shown in Fig. 6, dose dependence of the lattice parameter tends to saturate for all samples. The saturation occurrence is attributed to the lattice parameter increase with increasing number of lattice defects. The maximum lattice defect concentration might be limited and controlled by the temperature during radiation, the density and the grain size of samples. It should also be pointed out here that self-radiation damage causes a number of lattice defects, including some kinds of Frenkel pairs (Frenkel defects) and some of them are annealed by α-recoil causing a temperature rise of the corresponding region. The concept is also supported by Nellis [7]. Table 4 shows that values of A and B with MOX have good agreement with those of PuO_2.

4.2. Thermal recovery of self-radiation damage

As noted before, three kinds of lattice defects might be considered for MOX from Figs. 3 and 5. Consideration is given next to thermal recovery behavior as corresponding to the type of lattice defects of MOX. There are four types of lattice defects: anion Frenkel defects, cation Frenkel defects, defects composed of isolated helium trapped in a vacancy and spike defects caused by recoil ions produced by self-radiation. Since it can be considered that accumulation of spike defects does not cause lattice expansion, each of the three thermal recovery stages then corresponds to the recovery of anion Frenkel defects, cation Frenkel defects and defects composed of isolated helium trapped in a vacancy.

At first activation energy for recovery is calculated using thermal recovery experimental data according to the following procedure. It is assumed that recovery of the lattice parameter, $(a - a_{s,i})$, in each recovery stage is proceeded by a first order reaction according to the following equation:

$$\ln(a - a_{s,i}) = -K_i \times t + C_0, \tag{5}$$

where a is lattice parameter after annealing time; t, $a_{s,i}$ is saturated lattice parameter of recovery stage; i, K_i is rate constant of recovery stage; i, t is annealing time and C_0 is a constant. The lattice parameters recovery in the three recovery stages are estimated from Figs. 3 and 5 to be −0.0575% (0.25), −0.184% (0.80), −0.23% (1.0), respectively, because three kinds lattice defects are recovered on annealing at 673, 1073 and 1473 K, respectively. The relationship between $\ln(a - a_{s,i})$ and t for several temperatures can be easily obtained by the annealing experiment done here, then the K_i values are determined for each temperature. The activation energy, E, can be estimated from the following expression:

$$K_i = K_0 \exp(-E/kT),$$

where k is the Boltzmann constant, K_0 is a constant and T is temperature. The rate constant, K_i, is obtained as follows:

$$K_1 = 0.002 \exp(-1400/T), \tag{6}$$

$$K_2 = 0.80 \exp(-8500/T), \tag{7}$$

and

$$K_3 = 5.0 \exp(-14000/T). \tag{8}$$

Table 6
Comparison of activation energy.

	Temperature (K)	Activation energy (eV)	References
Thermal recovery of lattice expansion in MOX			This work
Stage I	<673	0.12	
Stage II	673–1073	0.73	
Stage III	1073–1573	1.2	
Thermal recovery of point defects in irradiated UO_2			
U_i in UO_2	<763	0.1–0.4	[18]
V_U in UO_2	853–1023	2.0–2.4	[19–21]
O_i in UO_2	373–673	0.9–1.4	[19–22]
V_O in UO_2	973–1073	1.7–2.8	[19,18]
Diffusion in MOX			
O in $MO_{2\pm X}$	473–1273	0.2–0.7	[23]
U in $MO_{2\pm X}$	1173–1873	1.6	[24,25]
Pu in $MO_{2\pm X}$	1173–1873	1.42	[24,25]

Thus the activation energies for Stage I, Stage II and Stage III are calculated as 0.12, 0.73 and 1.2 eV, respectively. The activation energies obtained here are compared with those in the literature [6,8,12,17] in Table 5. The activation energy of MOX for Stage I is in agreement with that of PuO_2, but it is smaller than that of UO_2. The activation energies of MOX for Stage II and Stage III are also smaller than those of UO_2 as shown in Table 5. The difference in thermal recovery behavior between MOX and UO_2 might be due to the characteristics of the samples such as pellet density and grain size which are related to sink density for interstitial atoms. In addition, the difference might be explained by the fact that MOX is composed of many cations having various ionic radii as discussed below.

Table 6 compares activation energies which correspond to thermal recovery of lattice expansion in MOX obtained in this study, thermal recovery of point defects in UO_2 [18–22] and diffusion of oxygen, uranium and plutonium ions in MOX [23–25]. As shown in Table 6, uranium interstitial type defects can be annealed around 763 K with an activation energy of 0.1–0.4 eV and oxygen ions can migrate with an activation energy of 0.2–0.7 eV in the temperature range from 473 to 1273 K. Since the lattice defects in the first recovery stage can be completely recovered at temperatures below 673 K with low activation energy of 0.12 eV, the first recovery stage is considered to correspond to the recovery of anion Frenkel defects that can be easily annihilated with the lowest activation energy among the three kinds of defects noted above. The total amount of helium gas atoms accumulated in the pellets during two years is estimated to be about 45 μl, and only 0.07 μl of helium can be detected at 1273 K and no release of helium gas atoms can be detected at 1373 K.

The result might be explained by the fact that helium gas atoms which are present very near the pellet surface can be released and the other helium gas atoms which are trapped by a vacancy in the lattice can be clustered into helium gas bubbles and they are trapped by pores in the pellet. Such helium gas bubbles cannot cause lattice expansion. Therefore, the third recovery stage is considered to correspond to the recovery of defects composed of

Table 7
The change ratio of lattice parameter in each stage (%).

	Total	Stage I	Stage II	Stage III
MOX	0.29	0.08	0.15	0.06
UO_2 [13]	0.84	0.29	0.30	0.25
$(U,Th)O_2$ [16]	0.55	0.25	0.22	0.08
PuO_2 [11]	0.34	0.15	0.13	0.06
PuO_2 [8]	0.32	0.13	0.14	0.05

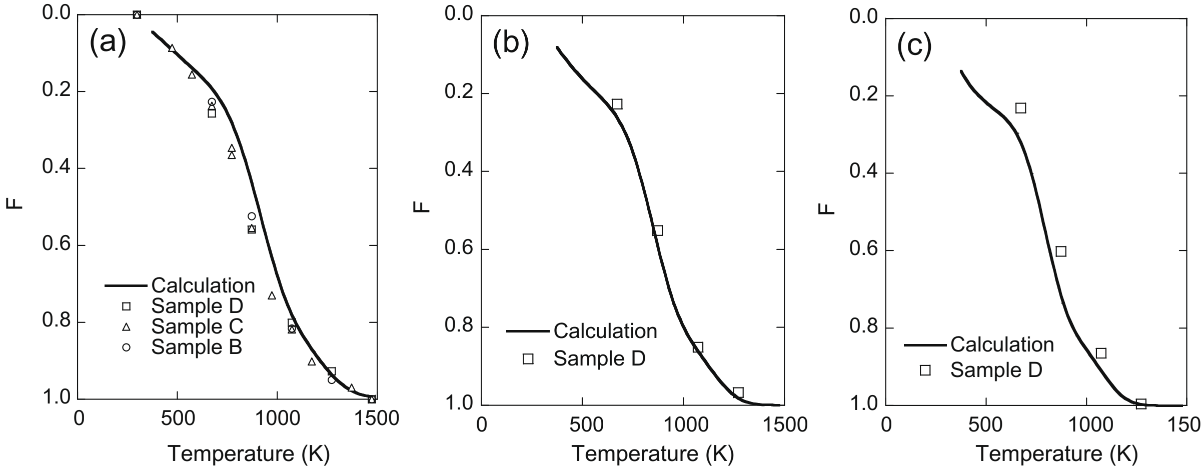

Fig. 7. Recovery fraction, *F*, after annealing for: (a) 2 h, (b) 4 h and (c) 8 h.

isolated helium trapped in a vacancy, and as a result, the second recovery stage is considered to correspond to the recovery of cation Frenkel defects. This speculation for the thermal recovery mechanism coincides with the results reported for UO_2 and $(U,Th)O_2$ [13,16]. The third thermal recovery stage with PuO_2 has not been discussed in the literature. However, the third recovery stage can be clearly found above 1073 K with PuO_2 in Fig. 4.

The lattice expansion of each recovery stage to the total lattice expansion is estimated from Figs. 3 and 5 and is summarized in Table 7. The data of UO_2, $(U,Th)O_2$ and PuO_2 are also shown there for comparison. The lattice expansions of three recovery stages with MOX are 0.08%, 0.15% and 0.06%, respectively. On the other hand, those of PuO_2 are 0.15–0.13%, 0.13–0.14% and 0.05–0.06%. This means that the contribution of oxygen Frenkel defects on lattice expansion in MOX is small compared with PuO_2. The contribution of metal Frenkel defects and defects composed of isolated helium trapped in a vacancy to lattice defects is almost the same for each.

It might be considered that oxygen interstitial atoms tend to increase the valence of cations and oxygen vacancies tend to decrease the valence, keeping electrical neutrality. This means that oxygen interstitial atoms promote the change of uranium ions from +4 to +5, and oxygen vacancies promote the change of plutonium ions from +4 to +3, and these changes cause the lattice expansion. The small contribution observed in the first recovery stage might be due to the fact explained above. In addition, it might be speculated that excess oxygen vacancy should cause the saturation of oxygen interstitial atoms at low concentration and the recovery with low activation energy if the MOX pellets used in this experiment have a low density and small grain size, i.e., high sink density for interstitial atoms. If this is true, the small fraction of lattice expansion and the small activation energy for recovery in the first stage can be easily accepted.

The recovery fractions *F* are calculated as a function of temperature and annealing time using Eqs. (5)–(8), and the calculation results are shown in Fig. 7 together with experimental data. The calculation reproduces the experimental data very well. The calculation results after annealing for 8 h shows recovery in three stages as shown in Fig. 7(c). These results show that the recovery stages are not observed clearly in the experimental data shown in Fig. 3, because annealing time was too short.

5. Conclusion

Self-radiation damage of α-particles in MOX was examined in this study. MOX samples stored for several decades remained in good condition and lattice parameter changes during storage and after annealing were measured in detail. The results obtained are summarized as follows.

(1) An empirical equation could be derived and the equation could predict the dependence of lattice parameter change on self-radiation dose. The lattice parameter saturated after expansion of about 0.29%.
(2) Three thermal recovery stages were observed and the mechanisms for these recoveries were considered to be due to the recoveries of anion Frenkel defects, cation Frenkel defects and defects composed of isolated helium trapped by a vacancy. Their corresponding activation energies were estimated to be 0.12, 0.73 and 1.2 eV, respectively.
(3) Lattice expansion due to self-radiation with MOX was small compared with those for UO_2 and PuO_2, and it was explained by the fact that lattice expansion of MOX due to oxygen interstitial atoms was smaller than that of other actinide oxides.

Acknowledgement

The authors are pleased to acknowledge Mr. T. Tamura for their collaboration in the sample preparation.

References

[1] M.H. Rand, A.C. Fox, R.S. Street, Nature 195 (1962) 565.
[2] R.O. Elliot, C.E. Olsen, J. Appl. Phys. 35 (6) (1964) 1925.
[3] K. Mendelssohn, E. King, J.A. Lee, M.H. Rand, C.S. Griffin, R.S. Street, Plutonium 1965, Barnes and Noble, New York, 1967. p. 189.
[4] H.E. Schmidt, J. Richter, H. Matzke, J. van Geel, in: Proceedings of the 22nd International Conference on Thermal Conductivity, 1994, p. 920.
[5] J. Leteurtre, Y. Quere, Irradiation Effects in Fissile Materials, E-Publishing Inc., New York, 1972.
[6] T.D. Chikalla, R.P. Turcotte, Radiat. Eff. 19 (1973) 93.
[7] W.J. Nellis, Inorg. Nucl. Chem. Lett. 13 (1977) 393.
[8] M. Noe, J. Fuger, Inorg. Nucl. Chem. Lett. 10 (1974) 7.
[9] W.C. Mosley, J. Am. Ceram. Soc. 54 (10) (1971) 475.
[10] C. Hurtgen, J. Fuger, Inorg. Nucl. Chem. Lett. 13 (1977) 179.
[11] R.P. Turcotte, Plutonium 1975 and Other Actinides, Elsevier, New York, 1976. p. 851.
[12] W.J. Weber, J. Nucl. Mater. 98 (1981) 206.
[13] W.J. Weber, J. Nucl. Mater. 114 (1983) 213.
[14] W.J. Weber, Radiat. Eff. 83 (1984) 145.
[15] K. Asakura, T. Yamaguchi, T. Ohtani, J. Nucl. Mater. 357 (2006) 126.
[16] R. Evron, G. Kimel, Y. Eyal, J. Nucl. Mater. 217 (1994) 54.
[17] I.I. Kapshukov, L.V. Sudakov, G.N. Yakovlev, Sov. Phys. – Solid State 12 (7) (1971) 1718.
[18] J. Soullard, French Commissariat à l' Energie Atomique Report, CEA-R-4882, 1977.

[19] H. Blank, Plutonium 1975 and Other Actinides, Elsevier, New York, 1976. p. 873.
[20] D. Vollath, Plutonium 1975 and Other Actinides, Elsevier, New York, 1976. p. 843.
[21] P. Nagels, W.V. Lierde, R. DeBatist, M. Denayer, L.D. Jonghe, R. Gevers, Thermodynamics, II IAEA, Vienna, 1966. p. 311.
[22] W. Breitung, J. Nucl. Mater. 74 (1978) 10.
[23] F. Dannucci, C. Sari, J. Nucl. Mater. 68 (1977) 357.
[24] A.S. Bayoglu, R. Renzelli, Solid State Ion. 12 (1984) 53.
[25] R. Lindner D. Reimann, F. Schmitz., Plutonium as a Reactor Fuel, IAEA, Vienna, 1967. p. 265.